

Regulation of Na⁺/H⁺ exchanger NHE3 by glucagon-like peptide 1 receptor agonist exendin-4 in renal proximal tubule cells

Luciene R. Carraro-Lacroix,^{1,3} Gerhard Malnic,¹ and Adriana C. C. Girardi^{1,2}

¹Department of Physiology and Biophysics, Institute of Biomedical Sciences; ²Heart Institute (InCor), Medical School, University of São Paulo, and ³Department of Physiology, Federal University of São Paulo, São Paulo, Brazil

Submitted 12 February 2009; accepted in final form 17 September 2009

Carraro-Lacroix LR, Malnic G, Girardi AC. Regulation of Na⁺/H⁺ exchanger NHE3 by glucagon-like peptide 1 receptor agonist exendin-4 in renal proximal tubule cells. *Am J Physiol Renal Physiol* 297: F1647–F1655, 2009. First published September 23, 2009; doi:10.1152/ajprenal.00082.2009.—The gut incretin hormone glucagon-like peptide 1 (GLP-1) is released in response to ingested nutrients and enhances insulin secretion. In addition to its insulinotropic properties, GLP-1 has been shown to have natriuretic actions paralleled by a diminished proton secretion. We therefore studied the role of the GLP-1 receptor agonist exendin-4 in modulating the activity of Na⁺/H⁺ exchanger NHE3 in LLC-PK₁ cells. We found that NHE3-mediated Na⁺-dependent intracellular pH (pH_i) recovery decreased ~50% after 30-min treatment with 1 nM exendin-4. Pharmacological inhibitors and cAMP analogs that selectively activate protein kinase A (PKA) or the exchange protein directly activated by cAMP (EPAC) demonstrated that regulation of NHE3 activity by exendin-4 requires activation of both cAMP downstream effectors. This conclusion was based on the following observations: 1) the PKA antagonist H-89 completely prevented the effect of the PKA activator but only partially blocked the exendin-4-induced NHE3 inhibition; 2) the MEK1/2 inhibitor U-0126 abolished the effect of the EPAC activator but only diminished the exendin-4-induced NHE3 inhibition; 3) combination of H-89 and U-0126 fully prevented the effect of exendin-4 on NHE3; 4) no additive effect in the inhibition of NHE3 activity was observed when exendin-4, PKA, and EPAC activators were used together. Mechanistically, the inhibitory effect of exendin-4 on pH_i recovery was associated with an increase of NHE3 phosphorylation. Conversely, this inhibition took place without changes in the surface expression of the transporter. We conclude that GLP-1 receptor agonists modulate sodium homeostasis in the kidney, most likely by affecting NHE3 activity.

dipeptidyl peptidase IV; sodium reabsorption; intracellular pH; protein kinase A; exchange protein directly activated by cAMP

NHE3 IS THE APICALLY LOCATED Na⁺/H⁺ exchanger that mediates the majority of NaCl and NaHCO₃ reabsorption in the renal proximal tubule (2, 42, 47, 48, 50). Numerous physiological and humoral factors regulate NHE3 activity, thereby contributing to the fine control of fluid and electrolyte homeostasis (1, 8, 12, 40, 46, 52).

To understand the molecular mechanisms underlying regulation of NHE3, there has been great interest in identifying proteins that associate with the transporter. We previously reported (13) that NHE3 and the serine protease dipeptidyl peptidase IV (DPPIV) reside together as an oligomeric complex in the renal proximal tubule. The functional role of DPPIV

in regulating NHE3 activity has been shown in OKP cells (a line of opossum proximal tubule cells) (15) and in the intact proximal tubule in vivo (14). We have demonstrated that highly specific competitive inhibitors that bind to the active site of DPPIV significantly reduce NHE3 function, suggesting that the DPPIV catalytic site has a tonic role in stimulating NHE3 (14, 15).

DPPIV is a multifunctional protein expressed on the surface of several cell types, including epithelial cells, endothelial cells, and lymphocytes (34). It selectively cleaves NH₂-terminal dipeptides from proteins having proline or alanine in amino acid position 2 (25, 34). DPPIV also acts as a binding protein (34) and signaling molecule (29, 34).

Currently, the molecular mechanisms by which DPPIV modulates NHE3 activity are not well understood. DPPIV is known to degrade a variety of peptide hormones, cytokines, and chemokines (34, 37). It is possible that DPPIV plays a tonic role in stimulating NHE3 by processing an inhibitory peptide involved in modulation of the transporter. The effect of DPPIV inhibition on NHE3 activity might thereby be mediated by increasing the half-life of this candidate peptide. One such candidate is the DPPIV substrate glucagon-like peptide 1 (GLP-1).

GLP-1 is a hormone produced in intestinal L-type cells and released into the bloodstream in response to ingested food (9, 23). It stimulates β-cell proliferation and insulin secretion in a glucose-dependent manner, suppresses glucagon secretion, inhibits gastric emptying, and reduces appetite and food intake (4, 9, 10, 23). As a result of such biological actions, GLP-1 is considered a potential therapeutic agent for type 2 diabetes. However, the usefulness of native GLP-1 is limited because of its rapid inactivation by DPPIV (7, 30). In contrast, exendin-4, a 39-amino acid peptide that shares 53% sequence homology with GLP-1, has a much higher in vivo half-life on account of its NH₂-terminal resistance to DPPIV cleavage (45). Exendin-4 was originally isolated from the salivary glands of the Gila monster (*Heloderma suspectum*), a poisonous lizard from the deserts of Arizona (11), and is now registered as an antidiabetic agent under the name of Byetta (4).

The effects of GLP-1 and exendin-4 are mediated after binding to a specific plasma membrane receptor of the G protein-coupled receptor family (GLP-1R). The GLP-1R is expressed not only in the pancreatic β-cell but also in the brain, the kidneys, the lungs, the pituitary gland, the heart, the stomach, the small intestine, and major blood vessels (10, 23, 41). This widespread distribution of the GLP-1R suggests that GLP-1 may exert a large variety of biological actions.

Animal studies indicate that GLP-1 has natriuretic and diuretic properties (35, 39, 51), and infusion studies in humans confirm these actions (19, 20), suggesting a potential role for

Address for reprint requests and other correspondence: A. C. C. Girardi, Institute of Heart—Laboratory of Genetics and Molecular Cardiology, Univ. of São Paulo Medical School, Avenida Dr. Enéas de Carvalho Aguiar, 44, 10^o andar, Bloco II, 05403-900 São Paulo, SP, Brazil (e-mail: adriana.girardi@incor.usp.br).

this peptide in sodium and water homeostasis. It is noteworthy that Gutzwiller and colleagues (20) found that intravenous infusion of GLP-1 into healthy and insulin-resistant obese subjects not only increases urinary sodium excretion but also reduces urinary proton secretion, implicating a role for GLP-1 in modulation of renal Na^+/H^+ exchange.

On the basis of these observations, the present study was undertaken to evaluate the role of the GLP-1R agonist exendin-4 in modulating the activity of NHE3 in the kidney proximal tubule. We demonstrate that exendin-4 significantly inhibits NHE3-mediated Na^+ -dependent intracellular pH (pH_i) recovery in LLC-PK₁ cells, supporting the notion that GLP-1R agonists modulate sodium homeostasis in the kidney, most likely by affecting NHE3 activity.

METHODS

Materials. The LLC-PK₁ cell line first described by Hull et al. (28) was obtained from the American Type Culture Collection (Manassas, VA). Dulbecco's modified Eagle's medium (DMEM), heat-inactivated fetal bovine serum, sodium pyruvate, and penicillin-streptomycin were purchased from GIBCO Invitrogen (Grand Island, NY). BCECF-AM was obtained from Molecular Probes (Eugene, OR). Exendin-4, exendin-9 and GLP-1 were from Bachem (Torrance, CA). HOE-694 and S3226 were gifts from Sanofi-Aventis (Frankfurt, Germany). The cAMP analogs 8-(4-chlorophenylthio)-2'-O-methyladenosine-3',5'-cyclic monophosphate (8-pCPT-2'-O-Me-cAMP) and *N*⁶-monobutyryladenine-3',5'-cyclic monophosphate (6MB-cAMP) were from BioLog Life Science Institute (Bremen, Germany). EZ-Link sulfo-NHS-SS-biotin as well as immunopure immobilized streptavidin were purchased from Pierce (Rockford, IL). Rabbit polyclonal anti-pSer/Thr (18) was purchased from Cell Signaling Technology (Beverly, MA). The monoclonal (MAb) anti-NHE3 antibody 2B9 (2) was kindly provided by Dr. Peter Aronson and Dr. Daniel Biemesderfer at Yale University. In a previous paper, we described (13) the development and characterization of MAb 1D11 to rabbit DPPIV. Horseradish peroxidase-conjugated goat anti-mouse and goat anti-rabbit secondary antibodies were purchased from Zymed laboratories (San Francisco, CA). All other materials were from Sigma-Aldrich (St. Louis, MO), if not stated otherwise.

Cell culture. Cell passages 2–10 were used in our experiments. LLC-PK₁ cells were maintained in 75-cm² tissue culture flasks in DMEM supplemented with 45 mM NaHCO_3 , 25 mM HEPES buffer, 0.1 mM sodium pyruvate, 0.01 mM nonessential amino acids, 10% (vol/vol) heat-inactivated fetal bovine serum, 100 U/ml penicillin, and 100 $\mu\text{g}/\text{ml}$ streptomycin. Cultures were incubated at 37°C in a humidified 5% CO_2 -air atmosphere. Cells were subcultured with $\text{Ca}^{2+}/\text{Mg}^{2+}$ -free phosphate-buffered saline and 0.25% trypsin-EDTA. The medium was replaced every 2 days. For experiments, cells were seeded onto tissue culture plates, grown to confluence, and serum starved for 24 h before studies.

RT-PCR. Total RNA was extracted from LLC-PK₁ cells with TRIzol reagent (Invitrogen) and from rat tissues (renal cortex, renal medulla, and pancreas) with guanidinium thiocyanate. The quality and quantity of RNA were assessed by spectrophotometry at 260 and 280 nm. First-strand cDNA synthesis was performed with SuperScript III reverse transcriptase according to the manufacturer's recommended protocols. The resulting cDNAs (50 ng each) were subjected to PCR using the degenerated oligonucleotide primers 5'-TGTACCGGT-TCTGCACRGCTGA-3' (forward) and 5'-AAGCGATGACCARS-GCGGAGA-3' (reverse). The degenerate primers for the amplification of GLP-1R cDNA were designed according to the conserved sequences between porcine (GenBank accession no. CV871385) and rat (GenBank accession no. NM_012728) genes. The expected size of the amplified DNA band was 189 bp. The amplification conditions consisted of initial denaturation (95°C for 5 min) followed by 30

cycles: 95°C for 30 s, 60°C for 30 s, 72°C for 1 min, with final extension at 72°C for 10 min. PCR products were detected with agarose gel electrophoresis.

cAMP assays. cAMP levels were measured by enzyme immunoassay (cAMP Direct Biotrak EIA, GE Healthcare) according to manufacturer's instructions. Experiments were performed in the presence of the phosphodiesterase inhibitor IBMX (1 mM).

Fluorescence microscopy measurement of pH_i . NHE activity was measured in LLC-PK₁ cells as the rate of Na^+ -dependent pH_i recovery after an acid load. Dual excitation ratio determinations from the fluorescent pH-sensitive probe BCECF were used to measure pH_i , as previously detailed (5). Briefly, cells were grown to confluence on glass slides, placed into a thermoregulated chamber, and mounted on an inverted epifluorescence microscope (Nikon, TMD). Next, they were loaded with 10 μM BCECF acetoxymethyl ester in Ringer solution (solution 1, Table 1) for 10 min. The acetoxymethyl ester form of BCECF enters the cell and is rapidly converted to the anionic-free acid form by intracellular esterases. After the loading period, the glass coverslips were rinsed with the control solution to remove the BCECF-containing solution for a few minutes and pre-pulsed with 20 mM NH_4Cl in HEPES-buffered control solution (solution 3, Table 1) at 37°C for subsequent acid loading. Fluorescence was measured by using 440 (pH insensitive) or 495 (pH sensitive) nm alternately as excitation wavelengths utilizing a xenon light source. Emission was measured at 530 nm by a photomultiplier-based fluorescence system (Georgia Instruments, PMT-4000) at time intervals of 5 s. pH_i was calibrated by equilibrating the cells with high- K^+ medium (solution 2, Table 1) titrated to defined pH values and containing 10 $\mu\text{g}/\text{ml}$ nigericin.

Cell pH recovery. Cell pH recovery was examined after the acidification of pH_i with the NH_4Cl pulse technique after 2-min exposure to 20 mM NH_4Cl (solution 3, Table 1) in the presence of external 145 mM Na^+ (solution 1, Table 1). In all experiments, we calculated the initial rate of pH recovery (dpH/dt , pH units/min) from the first 2 min after the start of the pH_i recovery curve by linear regression analysis.

Measurement of intracellular buffering capacity. In our system, intracellular buffering capacity (β_i) corresponds to the sum of the individual buffering powers of all cytosolic buffers, excluding $\text{HCO}_3^-/\text{CO}_2$. Hence, estimations of β_i were performed with HEPES-buffered solutions. β_i was determined with the technique described by Boyarsky et al. (3) and calculated as described by Weintraub and Machen (49). The H^+ membrane transporters were blocked by a Na^+ -free solution plus 0.1 μM concanamycin. After removal of Na^+ from the external medium, the cells were exposed to a HEPES-buffered solution containing 50 mM NH_4Cl , which was then stepwise reduced to 1 mM (in 50, 20, 10, 5, 2.5, and 1 mM steps). Calculation of β_i was

Table 1. Composition of solutions

Reagents	Solution 1	Solution 2	Solution 3
	Ringer	$\uparrow \text{K}^+$ Medium	NH_4Cl
NaCl	141.0	20.0	121.0
KCl	5.4	130.0	5.4
CaCl_2	1.0	1.0	1.0
KH_2PO_4	0.4		0.4
MgCl_2	0.5	1.0	0.5
MgSO_4	0.4		0.4
Na_2HPO_4	0.3		0.3
HEPES	10.0	5.0	10.0
Glucose	0.6		0.6
NH_4Cl			20.0
pH	7.4	6, 7, and 8	7.4

All values are in mM, except for pH. NMDG, *N*-methyl-D-glucamine. HCl or NaOH was used in all Na^+ -containing solutions to titrate to the appropriate pH, and KOH was used in the Na^+ -free solution.

performed according to the formula $\beta_i = \Delta[\text{NH}_4^+]_i / \Delta\text{pH}_i$, where the intracellular NH_4^+ concentration ($[\text{NH}_4^+]_i$) was calculated from the Henderson-Hasselbalch equation on the assumption that $\text{NH}_{3i} = \text{NH}_3$.

Immunoprecipitation. LLC-PK₁ cells grown in six-well plates were solubilized at 4°C in a modified RIPA buffer containing 150 mM NaCl, 5 mM EDTA, 1% (vol/vol) Triton X-100, 0.5% (wt/vol) deoxycholate, 50 mM Tris·HCl, pH 7.4, supplemented with protease inhibitors (0.7 μg/ml pepstatin A, 0.5 μg/ml leupeptin, and 40 μg/ml PMSF) and phosphatase inhibitors (50 mM NaF and 15 mM sodium pyrophosphate). The samples were subjected to centrifugation (14,000 g for 10 min) with a table top centrifuge (Eppendorf model 5402R). Fifty micrograms of primary antibodies was added to the supernatants, and the samples were incubated at 4°C for 1 h. Immune complexes were collected with 5 mg/sample of protein G-Sepharose 4B (GE Healthcare). The beads were washed five times in modified RIPA buffer and then prepared for SDS-PAGE and immunoblotting.

Cell surface biotinylation. The assay was performed as described previously (15). Cells were rinsed twice in ice-cold PBS-Ca-Mg (PBS with 0.1 mM CaCl₂, 1.0 mM MgCl₂). Surface membrane proteins were then biotinylated by incubating the cells twice for 25 min with 2 ml of ice-cold biotinylation buffer (150 mM NaCl, 10 mM triethanolamine, 2 mM CaCl₂, and 2 mg/ml EZ-Link sulfo-NHS-SS-biotin). Cells were then rinsed twice for 20 min with a quenching buffer (PBS-Ca-Mg, 100 mM glycine), washed twice with ice-cold PBS-Ca-Mg, and scraped into ice-cold solubilization buffer (50 mM Tris, 150 mM NaCl, 1 mM EDTA, 0.5% sodium deoxycholate, 1% Triton X-100, pH 7.4) containing protease inhibitors (0.7 μg/ml pepstatin A, 0.5 μg/ml leupeptin, and 40 μg/ml PMSF). After lysis on ice for 60 min, extracts were centrifuged for 10 min at 14,000 g and 4°C. The protein concentration of the supernatants was measured (36), and equal protein amounts of cell lysate (500 μg) were equilibrated with streptavidin-agarose beads at 4°C. The beads were then washed five times in ice-cold solubilization buffer. Biotinylated proteins were released by incubation in Laemmli buffer and subjected to SDS-PAGE and immunoblotting.

SDS-PAGE and immunoblotting. Proteins were solubilized in sample buffer (2% SDS, 20% glycerol, 100 mM dithiothreitol, 50 mM Tris pH 6.8, 0.05% bromophenol blue) and separated by SDS-PAGE using 7.5% polyacrylamide gels. Proteins were then transferred from the polyacrylamide gel to a polyvinylidene difluoride (PVDF) microporous membrane (Immobilon-P; Millipore, Bedford, MA) that was used for immunoblotting. The PVDF membrane was incubated with blocking solution [5% nonfat dry milk and 0.1% Tween 20 in PBS, pH 7.4 or 5% albumin and 0.1% Tween 20 in Tris-buffered saline (TBS) buffer, pH 7.4, when probing with anti-pSer/Thr antibody] for 1 h at room temperature to block nonspecific binding, followed by overnight incubation at 4°C with the primary antibody in blocking solution. The membranes were then washed five times in blocking solution and incubated for 1 h with horseradish peroxidase-conjugated IgG secondary antibodies from Zymed Laboratories (1:2,000). Membranes were again washed with blocking solution and then rinsed with PBS or TBS. Bound antibody was detected with enhanced chemiluminescence (ECL) (GE Healthcare, Piscataway, NJ) according to manufacturer's protocols. Multiple exposures of Kodak BioMax MR Film (Kodak, Rochester, NY) were made to ensure that signals were within the linear range of the film. The visualized bands were digitized with the ImageScanner (GE Healthcare) and quantified with Scion Image Software (Scion, Frederick, MD).

Statistics. All results are reported as means ± SE, with *n* indicating the number of observations. Comparisons between two groups were performed with unpaired *t*-tests. If more than two groups were compared, statistical significance was determined by ANOVA followed by Tukey's post hoc test. A *P* value <0.05 was considered significant. The Graph Pad Prism 4 program (Graph Pad Software, San Diego, CA) was used to calculate significance.

RESULTS

Expression of glucagon-like peptide 1 receptor in LLC-PK₁ cells. Expression of mRNA encoding GLP-1R was examined by means of RT-PCR and DNA sequencing analyses. GLP-1R mRNA was expressed in LLC-PK₁ cells and rat renal cortex; rat pancreas cDNA was used as positive control. In contrast, GLP-1R message was not detected in the rat renal medulla (Fig. 1A).

The GLP-1R is a G protein-coupled receptor whose activation by ligands stimulates the formation of intracellular cAMP (10, 16, 17). As shown in Fig. 1B, LLC-PK₁ cell treatment with 1 nM exendin-4 for 30 min significantly increased the intracellular levels of cAMP. The GLP-1R antagonist exendin-9 (16, 43) alone did not alter intracellular cAMP production but

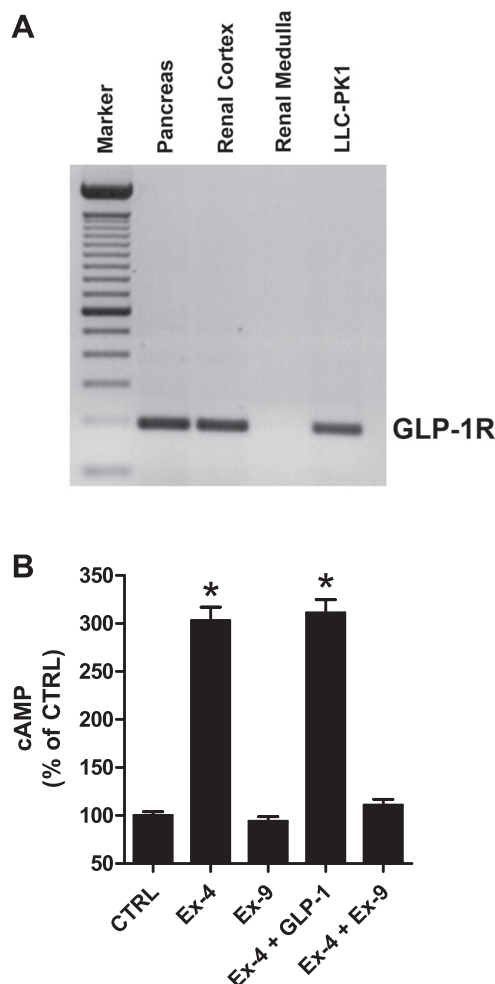


Fig. 1. Functional expression of glucagon-like peptide 1 receptor (GLP-1R) in LLC-PK₁ cells. **A:** RT-PCR detection of GLP-1R in rat pancreas, rat renal cortex, rat renal medulla, and LLC-PK₁ cells. Total RNA was extracted from rat tissues and LLC-PK₁, reverse transcribed, and amplified by PCR as described in METHODS. After PCR amplification, a single band with the predicted size (189 bp) was clearly detected in rat islets, rat renal cortex, and LLC-PK₁ cDNAs. **B:** effects of exendin-4 (Ex-4; 1 nM), exendin-9 (Ex-9; 1 μM), and combination of exendin-4 with exendin-9 on generation of intracellular cAMP in LLC-PK₁ cells. Cells were treated with the above-mentioned drugs for 30 min at 37°C. cAMP levels were measured by enzyme immunoassay (cAMP Direct Biotrak EIA, GE Healthcare) according to manufacturer's instructions. Each assay was performed in triplicate, and the mean values of 5 assays were calculated. **P* < 0.001 vs. control (Ctrl).

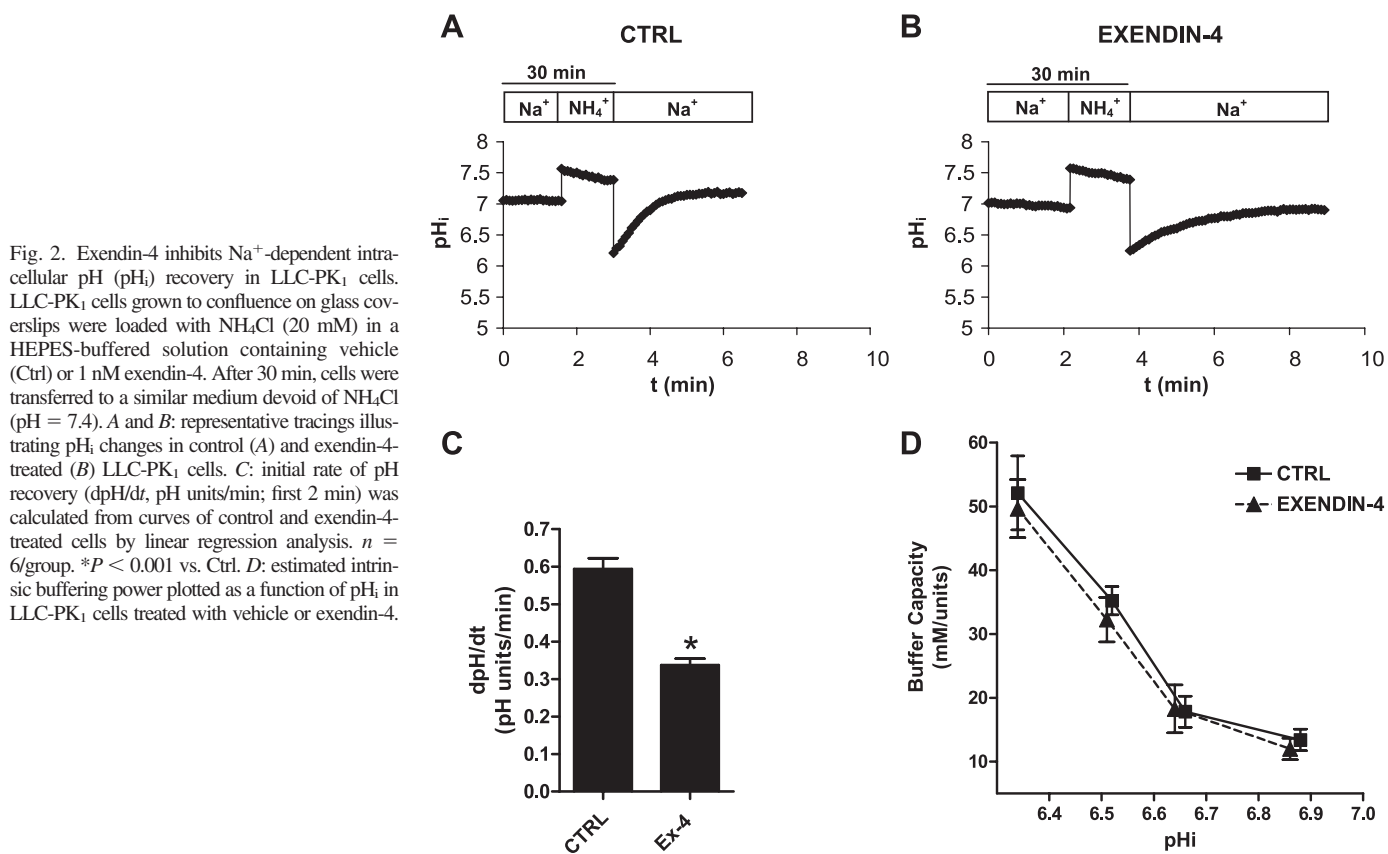


Fig. 2. Exendin-4 inhibits Na⁺-dependent intracellular pH (pH_i) recovery in LLC-PK₁ cells. LLC-PK₁ cells grown to confluence on glass coverslips were loaded with NH₄Cl (20 mM) in a HEPES-buffered solution containing vehicle (Ctrl) or 1 nM exendin-4. After 30 min, cells were transferred to a similar medium devoid of NH₄Cl (pH = 7.4). A and B: representative tracings illustrating pH_i changes in control (A) and exendin-4-treated (B) LLC-PK₁ cells. C: initial rate of pH recovery (dpH/dt, pH units/min; first 2 min) was calculated from curves of control and exendin-4-treated cells by linear regression analysis. *n* = 6/group. **P* < 0.001 vs. Ctrl. D: estimated intrinsic buffering power plotted as a function of pH_i in LLC-PK₁ cells treated with vehicle or exendin-4.

completely inhibited the effect of exendin-4. No additive effect on cAMP levels was observed when LLC-PK₁ cells were treated with a combination of GLP-1 and exendin-4 compared with cells treated with exendin-4 alone. These results strongly suggest that exendin-4 functionally interacts with its receptor in LLC-PK₁ cells.

Modulation of NHE3 activity by exendin-4 in LLC-PK₁ cells. To determine whether exendin-4 modulates NHE3 activity, we examined the effect of this peptide on Na⁺-dependent pH_i recovery from an acid load in LLC-PK₁ cells by using the NH₄Cl pulse technique. Representative tracings of pH_i changes in LLC-PK₁ cells treated with vehicle or exendin-4 are shown in Fig. 2, A and B, respectively. LLC-PK₁ cells were acidified to a pH_i of ~6.4, and the rates of pH_i recovery were determined in the presence of external Na⁺. As shown in Fig. 2C, the Na⁺-dependent pH_i recovery rates were significantly slower in exendin-4-treated cells (0.34 ± 0.02 pH units/min) than in controls (0.53 ± 0.07 pH units/min). We also determined the H⁺ buffering power in LLC-PK₁ cells treated or not with exendin-4 to rule out that the effect of this peptide on dpH/dt was due to alterations in the intracellular intrinsic buffering capacity β_i. β_i was estimated over the range 6.3–7.0 with stepwise reduction of external NH₄Cl. The resulting estimates of β_i at various values of pH_i are illustrated in Fig. 2D. Our data revealed no difference in β_i between control and exendin-4-treated LLC-PK₁ cells.

Because LLC-PK₁ cells express both NHE1 and NHE3 isoforms, we next sought to examine whether the decreased Na⁺-dependent pH_i recovery induced by exendin-4 was due to inhibition of NHE1 and/or NHE3 activity. For this purpose,

experiments were performed with 10 μM HOE-694 and 10 μM S3226, to inhibit selectively NHE-1 and NHE-3 isoforms, respectively. As seen in Fig. 3, HOE-694 inhibited ~50% of total Na⁺-dependent pH_i recovery in LLC-PK₁ cells (0.24 ± 0.02 pH units/min). The HOE-694-insensitive rate of pH_i recovery could be reduced still more by exendin-4 (0.11 ± 0.01 pH units/min). Conversely, no difference was found

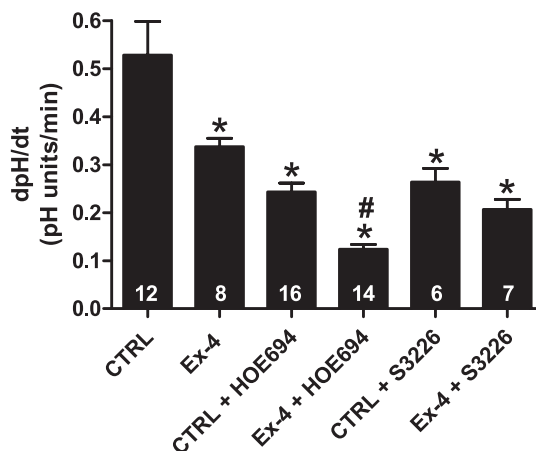


Fig. 3. Exendin-4 inhibits Na⁺/H⁺ exchanger (NHE)3-mediated Na⁺-dependent pH_i recovery in LLC-PK₁ cells. LLC-PK₁ cells grown to confluence on glass coverslips were treated for 30 min with vehicle (Ctrl) or 1 nM exendin-4 in the presence or absence of specific NHE isoform inhibitors. Initial rate of Na⁺-dependent pH_i recovery after cellular acidification with the NH₄Cl pulse technique was measured as described in METHODS. Number of experiments is indicated in bars. **P* < 0.001 vs. Ctrl; #*P* < 0.05 vs. HOE-694.

between cells exposed to S3226 in the presence (0.26 ± 0.03 pH units/min) or absence (0.21 ± 0.02 pH units/min) of exendin-4, suggesting that the HOE-694-sensitive S3226-resistant NHE1 isoform is not modulated by exendin-4.

Together these findings provide strong evidence that exendin-4 decreases Na^+ -dependent pH_i recovery rates from cell acidification in LLC-PK₁ cells by inhibiting NHE3-mediated Na^+/H^+ exchange activity.

In all subsequent functional studies, 10 μM HOE-694 was used to inhibit NHE1.

Role of cAMP signaling pathway in regulation of NHE3 by exendin-4 in LLC-PK₁ cells. As noted above, exposure of LLC-PK₁ cells to 1 nM exendin-4 leads to significant increases in intracellular cAMP. We therefore examined whether the effect of exendin-4 on NHE3 in kidney proximal tubule cells depends on components of the cAMP signaling pathway. The data presented in Fig. 4 show that the membrane-permeant cAMP analog 8-bromoadenosine 3',5'-cyclic monophosphate (8-BrcAMP; 100 μM) caused a decrement in the initial rates of Na^+ -dependent pH_i recovery very similar in magnitude to that caused by exendin-4 (0.12 ± 0.02 vs. 0.11 ± 0.02 pH units/min). Furthermore, the effects of exendin-4 and 8-BrcAMP were not additive (0.12 ± 0.03 pH units/min).

As intracellular cAMP accumulates and subsequently increases protein kinase A (PKA) activity, we further addressed the involvement of this kinase in the exendin-4-mediated NHE3 inhibition in LLC-PK₁ cells. As summarized in Fig. 5, pretreatment with the PKA inhibitor H-89 (1 μM) had no intrinsic effects on pH_i responses (0.28 ± 0.02 vs. 0.25 ± 0.02 pH units/min) but fully prevented the inhibitory effect of the PKA activator 6MB-cAMP (0.25 ± 0.03 vs. 0.13 ± 0.02 pH units/min). Alternatively, H-89 significantly but not completely blocked the inhibitory effect of exendin-4 on NHE3-mediated pH_i recovery in LLC-PK₁ cells (0.19 ± 0.01 vs. 0.11 ± 0.03 pH units/min; $P < 0.01$), strongly suggesting that an additional mechanism is involved in modulation of NHE3 by exendin-4.

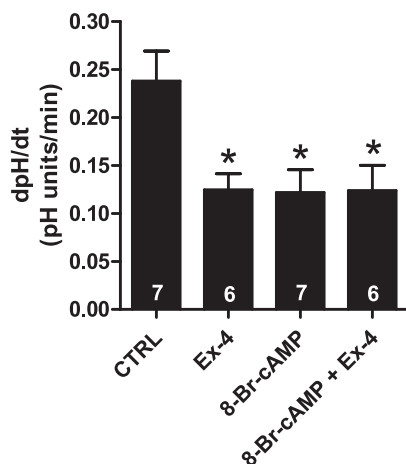


Fig. 4. cAMP mediates exendin-4-induced NHE3 inhibition in LLC-PK₁ cells. LLC-PK₁ cells grown to confluence on glass coverslips were incubated with 1 nM exendin-4, 100 μM 8-bromoadenosine 3',5'-cyclic monophosphate (8-BrcAMP), 1 nM exendin-4 + 100 μM 8-BrcAMP, or vehicle. The HOE-694-insensitive component of Na^+ -dependent pH_i recovery was measured in LLC-PK₁ cells by the NH_4Cl pulse technique. Number of experiments is indicated in bars. * $P < 0.001$ vs. Ctrl.

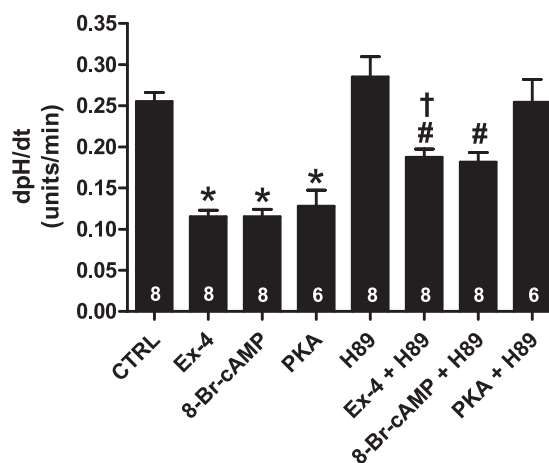


Fig. 5. Inhibitory effect of exendin-4 on NHE3 in LLC-PK₁ cells is partially mediated by protein kinase A (PKA). Confluent LLC-PK₁ cells were preincubated or not with the PKA inhibitor H-89 (1 μM) for 30 min before and during treatment with 1 nM exendin-4, 100 μM 8-BrcAMP, 50 μM PKA activator, or vehicle. The HOE-694-insensitive component of Na^+ -dependent pH_i recovery was measured in LLC-PK₁ cells by the NH_4Cl pulse technique. Number of experiments is indicated in bars. * $P < 0.001$ vs. Ctrl; # $P < 0.05$ vs. Ctrl; † $P < 0.01$ vs. exendin-4.

Exchange protein directly activated by cAMP (EPAC) is a recently discovered cAMP sensor that mediates intracellular cAMP actions in addition to the classic PKA cascade (6). Data from the literature demonstrated that EPAC mediates the cAMP-dependent guanine nucleotide exchange that activates Rap-1 (6). Activation of Rap-1 stimulates the kinase activity of B-Raf and the phosphorylation of mitogen-activated protein kinases MEK1/2 that subsequently phosphorylates and activates ERK1/2 (26). Since there are no available EPAC antagonists, the contribution of this pathway to the exendin-4-induced NHE3 inhibition was examined by using a cAMP analog that specifically activates EPAC (8-pCPT-2'-O-Me-cAMP) and the compound U-0126, an inhibitor of its downstream effector MEK1/2 kinase. As depicted in Fig. 6A, EPAC stimulation decreased NHE3-dependent pH_i recovery in LLC-PK₁ cells (0.13 ± 0.01 pH units/min). Preincubation for 30 min with U-0126 (50 μM) had no intrinsic effects on pH_i compared with control (0.26 ± 0.01 vs. 0.25 ± 0.02 pH units/min) but totally prevented the inhibitory effect of EPAC on NHE3 activity (0.25 ± 0.03 vs. 0.13 ± 0.01 pH units/min). In contrast, U-0126 curtailed but did not abolish the exendin-4 effect (0.20 ± 0.01 pH units/min). Since MEK1/2 may also be activated by PKA, we tested whether U-0126 would prevent the effect of PKA activation on NHE3 activity. A tendency to decrease the NHE3 inhibition generated by PKA was noted in the presence of U-0126, but it did not reach statistical significance (data not shown).

Further evidence implicating both PKA and EPAC pathways in mediating the exendin-4-induced inhibition of NHE3 is provided in Fig. 6B. The pretreatment of LLC-PK₁ with both H-89 and U-0126 abolished the exendin-4 effect. Additionally, no synergistic effect on the reduction of NHE3 activity is observed when LLC-PK₁ cells are treated simultaneously with exendin-4 and the cAMP analogs that selectively activate PKA or EPAC.

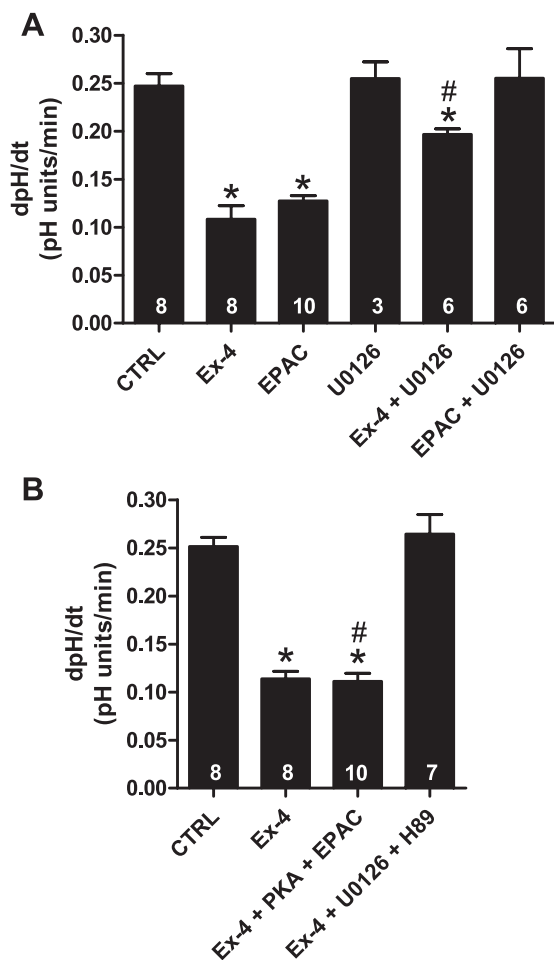


Fig. 6. Exendin-4-induced NHE3 inhibition in LLC-PK₁ cells occurs through both PKA- and exchange protein directly activated by cAMP (EPAC)-dependent mechanisms. *A*: confluent LLC-PK₁ cells were preincubated or not with the MEK1/2 inhibitor U-0126 (50 μ M) for 30 min before and during treatment with 1 nM exendin-4, 50 μ M EPAC activator, or vehicle. *B*: confluent LLC-PK₁ cells were preincubated or not with the PKA inhibitor H-89 (1 μ M) and with the MEK1/2 inhibitor U-0126 (50 μ M) for 30 min before and during treatment with 1 nM exendin-4. Another series of experiments were performed by treating cells with 1 nM exendin-4, 50 μ M PKA activator, and 50 μ M EPAC activator. The HOE-694-insensitive component of Na⁺-dependent pH_i recovery was measured in LLC-PK₁ cells by the NH₄Cl pulse technique. Number of experiments is indicated in bars. **P* < 0.001 vs. Ctrl; #*P* < 0.001 vs. Ex-4.

Collectively, these findings suggest that regulation of NHE3 activity in LLC-PK₁ cells by the GLP-1R agonist exendin-4 occurs through both PKA- and EPAC-dependent mechanisms.

Molecular mechanisms underlying acute regulation of NHE3 by exendin-4. Several studies have shown that cAMP-dependent PKA phosphorylates COOH-terminal NHE3 (27, 31–33, 38, 53). We therefore examined whether PKA activation induced by exendin-4 led to increased NHE3 phosphorylation. To this end, LLC-PK₁ cells were pretreated or not with the PKA inhibitor H-89, followed by addition of exendin-4, 8-BrcAMP, or vehicle. Cells were solubilized, and the resulting supernatant was immunoprecipitated with an antibody directed to NHE3 (MAb 2B9). The levels of NHE3 phosphorylation were then analyzed by immunoblotting using an anti-pSer/Thr antibody (18). As shown in Fig. 7, exendin-4, 8-BrcAMP, and the PKA activator 6MB-cAMP induced a

significant increase of NHE3 phosphorylation levels [$123 \pm 9\%$ ($n = 6$), $160 \pm 25\%$ ($n = 6$), and $144 \pm 23\%$ ($n = 3$), respectively] compared with control. As expected, pretreatment with H-89 completely prevented increases of NHE3 phosphorylation induced by these agents.

Consistent with previous findings (27), Kocinsky and co-workers (31) recently reported that phosphorylation of NHE3 at PKA consensus sites precedes transport inhibition, suggesting that phosphorylation per se is not sufficient to inhibit NHE3 activity. The authors postulated that PKA phosphorylation may subsequently result in NHE3 inhibition by altering NHE3 subcellular trafficking and/or modulating the interaction with regulatory proteins (31). To investigate whether the effect of exendin-4 to reduce NHE3 activity is due to changes in NHE3 surface expression, we performed cell surface biotinylation. The biotinylated surface proteins were precipitated on strepta-

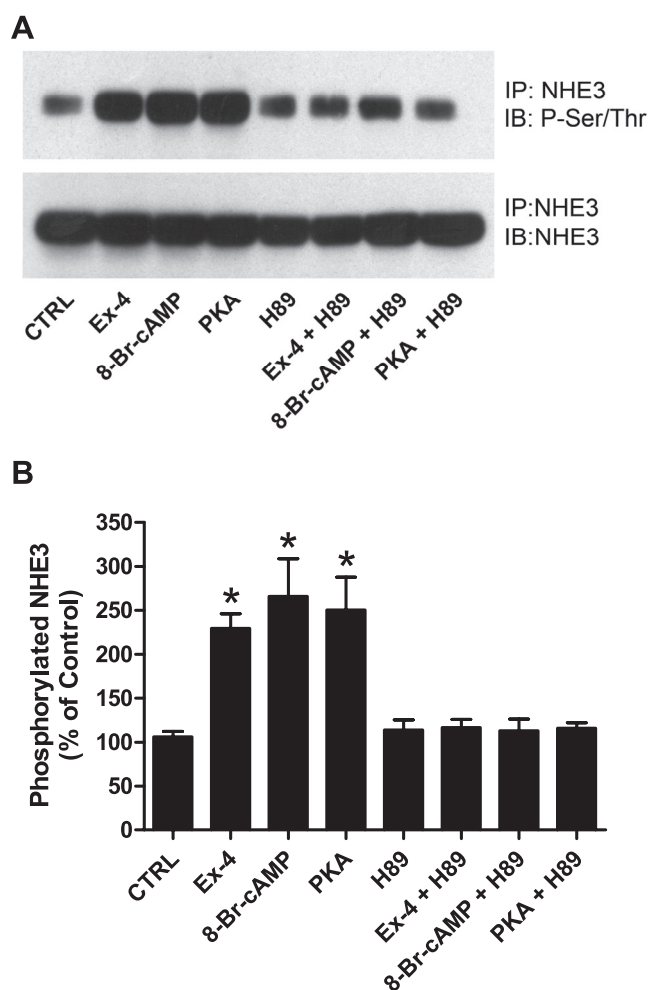


Fig. 7. Exendin-4 increases phosphorylation of NHE3 in LLC-PK₁ cells. *A*: Confluent LLC-PK₁ cells were preincubated or not with the PKA inhibitor H-89 (1 μ M) for 30 min before and during treatment with 1 nM exendin-4, 100 μ M 8-BrcAMP, 50 μ M PKA activator, or vehicle. Solubilized LLC-PK₁ protein extracts (500 μ g) were then immunoprecipitated (IP) with anti-NHE3. Immune complexes were prepared for immunoblotting (IB) and probed with an anti-pSer/Thr antibody. The blot was then stripped and probed with anti-NHE3 to show that equal amounts of NHE3 were immunoprecipitated in each lane. *B*: relative abundance of phosphorylated NHE3 was quantitated by densitometry and the combined data from 3 experiments are represented. **P* < 0.001 vs. Ctrl.

vidin followed by immunoblotting analysis of NHE3. As shown in Fig. 8, exendin-4 had no significant effect on NHE3 surface expression in LLC-PK₁ cells.

We next tested whether increases of NHE3 phosphorylation induced by exendin-4 would affect the stability of the NHE3-DPPIV complex. To this end, LLC-PK₁ cells incubated in the presence of exendin-4 or vehicle were solubilized and the resulting supernatant was immunoprecipitated with anti-DPPIV (MAb 1D11). The immune complexes were analyzed for the presence of NHE3 by immunoblotting. As seen in Fig. 9, exendin-4 treatment did not alter the amount of NHE3 in the DPPIV immune complex.

On the basis of these results, we conclude that acute treatment of LLC-PK₁ cells with exendin-4 increases NHE3 phosphorylation levels. The inhibitory effect of exendin-4 on NHE3 function is not associated with changes of NHE3 surface expression and occurs without affecting the assembly between NHE3 and DPPIV.

DISCUSSION

The potential role of GLP-1 and exendin-4 in modulating salt and water homeostasis has recently been reported in a series of elegant studies (19, 20, 22, 35, 39, 51). However, the assumption that GLP-1 reduces renal sodium reabsorption by affecting NHE3 activity is mainly based on indirect evidence. In the present study we demonstrate for the first time that the GLP-1R agonist exendin-4 inhibits NHE3-mediated Na⁺/H⁺ exchange in renal proximal tubule cells. Additionally, our data suggest that binding of exendin-4 to GLP-1R in LLC-PK₁ cells endogenously activates two cAMP downstream effectors, PKA and EPAC.

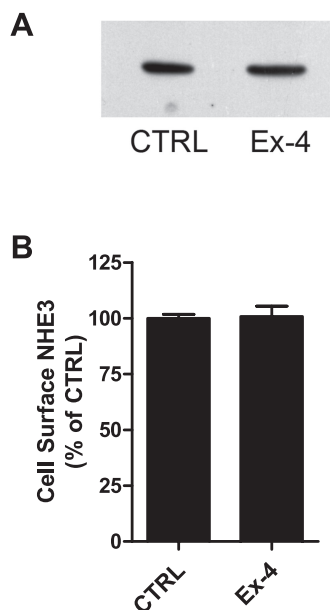


Fig. 8. Exendin-4 does not change NHE3 surface expression in LLC-PK₁ cells. *A*: confluent LLC-PK₁ cells were treated for 30 min with vehicle (Ctrl) or 1 nM exendin-4. Cell surface biotinylated proteins were subjected to SDS-PAGE and immunoblotting. Western blot analyses were performed with a monoclonal antibody against NHE3. *B*: abundance of NHE3 antigen was quantitated by densitometry, and the combined data from 4 experiments are represented.

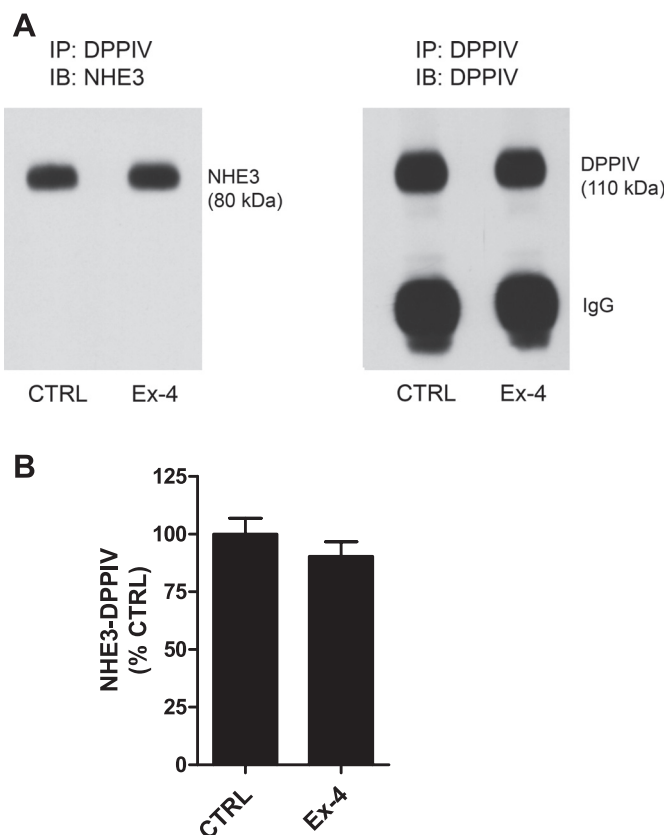


Fig. 9. Exendin-4 does not affect the stability of the NHE3-dipeptidyl peptidase IV (DPPIV) complex in LLC-PK₁ cells. Confluent LLC-PK₁ cells were treated with 1 nM exendin-4 or vehicle for 30 min. Equivalent quantities (500 μ g) of solubilized LLC-PK₁ cells were immunoprecipitated with an anti-DPPIV antibody. All incubation and washing solutions contained 1 nM exendin-4. *A*: immune complexes were prepared for immunoblotting, and the blot was probed with a monoclonal antibody directed to NHE3. To determine loading the blot was stripped and reprobed with an anti-DPPIV antibody. *B*: relative abundance of the NHE3-DPPIV complex was quantitated by densitometry, and the combined data from 3 experiments are represented.

The role of EPAC in regulation of NHE3 activity has been recently shown by Honegger and colleagues (24). However, the mechanism by which EPAC activation leads to NHE3 inhibition is still elusive. Here we demonstrate that LLC-PK₁ cell pretreatment with the MEK1/2 inhibitor U-0126 abolished the effect of the EPAC activator and diminished the exendin-4-induced NHE3 inhibition. Unexpectedly, neither exendin-4 nor EPAC activation changed the phosphorylation status of the MEK1/2 substrate ERK1/2 in LLC-PK₁ cells (data not shown). One possible way to reconcile these findings is by postulating that the effect of EPAC on NHE3 involves phosphorylation of a still unidentified protein by MEK1/2.

Biochemical and physiology studies have established the important role of PKA phosphorylation in regulating NHE3 activity (27, 31–33, 38, 53). Nonetheless, there is evidence from both in vitro (27) and in vivo (31) studies that phosphorylation per se is insufficient to inhibit NHE3. In the present report, we found that exendin-4 increases NHE3 phosphorylation without affecting NHE3 surface expression or its association with DPPIV. The subsequent events that lead to NHE3 inhibition may involve the association of NHE3 with other binding partners or yet unidentified mechanisms.

Our earlier studies demonstrated that NHE3 and DPPIV reside together in multimeric complexes in the renal brush-border membrane (13) and that specific competitive inhibitors that bind to the active site of DPPIV significantly reduce NHE3-mediated NaHCO_3 reabsorption in the rat renal proximal tubule (14). On the basis of our present and previous observations, we propose the following model to explain the role of GLP-1 in mediating the functional interaction between NHE3 and DPPIV in the intact proximal tubule in vivo. Inhibition of DPPIV activity by specific competitive inhibitors increases the levels of GLP-1 in the bloodstream and consequently in the glomerular ultrafiltrate. In the renal proximal tubule, GLP-1 binds to its receptor GLP-1R, increasing the intracellular levels of cAMP, leading, in turn, to cAMP-dependent activation of the PKA and EPAC pathways. Subsequent inhibition of NHE3-mediated Na^+/H^+ exchange in proximal tubule decreases sodium, bicarbonate, and water reabsorption. This hypothetical model is consistent with human studies in which GLP-1 infusions enhanced urinary sodium excretion and decreased proton secretion in healthy volunteers and in patients with type 2 diabetes (20).

The association of NHE3 with DPPIV, and the fact that this peptidase processes the peptide GLP-1 that is involved in regulation of the transporter, raises the possibility that NHE3, DPPIV, and the GLP-1R are linked together to form a functional unit. Of note, Herrera and coworkers (21) have reported that DPPIV interacts with the chemokine receptor CXCR4 in lymphocytes, in which the DPPIV-CXCR4 complex seems to play a role in immune system function and the pathophysiology of human immunodeficiency virus (HIV) infection. Binding of the CXCR4 ligand stromal cell-derived factor 1- α (SDF-1 α) to its receptor results in cointernalization of CXCR4 and DPPIV. SDF-1 α is a substrate of DPPIV, and when this peptidase is expressed on the cell surface SDF-1 α is cleaved and inactivated (39). The association between DPPIV and CXCR4 illustrates a regulatory mechanism that implicates both catalytic and binding properties of DPPIV. By analogy, it is possible that NHE3, DPPIV, and the GLP-1R physically and functionally interact in the renal brush-border membrane to regulate salt and water homeostasis. Unfortunately, we were unable to investigate whether a physical interaction between these proteins exists in LLC-PK₁ because specific GLP-1R antibodies suitable for immunoprecipitation and/or immunoblotting in LLC-PK₁ cells are not available.

In summary, we have found that the GLP-1R agonist exendin-4 reduces NHE3 activity in renal proximal tubule cells. This effect is mediated via PKA and EPAC signaling pathways and is associated with increased levels of NHE3 phosphorylation. The inhibition of DPPIV may enhance the renal effects of GLP-1, and might explain why DPPIV inhibitors decrease NHE3-mediated NaHCO_3 reabsorption in the rat renal proximal tubule.

GRANTS

This work was supported by Fundação de Amparo à Pesquisa do Estado de São Paulo (FAPESP) Grants 07/52945-8 (to A. C. C. Girardi) and 04/01683-5 (to G. Malnic) and by Conselho Nacional de Desenvolvimento Científico e Tecnológico (CNPq). L. R. Carraro-Lacroix was a recipient of a Postdoctoral Fellowship from FAPESP.

DISCLOSURES

No conflicts of interest are declared by the authors.

REFERENCES

- Ambuhl PM, Amemiya M, Danczkay M, Lotscher M, Kaissling B, Moe OW, Preisig PA, Alpern RJ. Chronic metabolic acidosis increases NHE3 protein abundance in rat kidney. *Am J Physiol Renal Physiol* 271: F917–F925, 1996.
- Biemesderfer D, Rutherford PA, Nagy T, Pizzonia JH, Abu-Alfa AK, Aronson PS. Monoclonal antibodies for high-resolution localization of NHE3 in adult and neonatal rat kidney. *Am J Physiol Renal Physiol* 273: F289–F299, 1997.
- Boyarsky G, Ganz MB, Sterzel RB, Boron WF. pH regulation in single glomerular mesangial cells. I. Acid extrusion in absence and presence of HCO_3^- . *Am J Physiol Cell Physiol* 255: C844–C856, 1988.
- Campbell RK, White JR Jr. More choices than ever before—emerging therapies for type 2 diabetes. *Diabetes Educ* 34: 518–534, 2008.
- Carraro-Lacroix LR, Ramirez MA, Zorn TM, Rebouças NA, Malnic G. Increased NHE1 expression is associated with serum deprivation-induced differentiation in immortalized rat proximal tubule cells. *Am J Physiol Renal Physiol* 291: F129–F139, 2006.
- de Rooij J, Zwartkruis FJ, Verheijen MH, Cool RH, Nijman SM, Wittinghofer A, Bos JL. Epac is a Rap1 guanine-nucleotide-exchange factor directly activated by cyclic AMP. *Nature* 396: 474–477, 1998.
- Deacon CF, Nauck MA, Toft-Nielsen M, Pridal L, Willms B, Holst JJ. Both subcutaneously and intravenously administered glucagon-like peptide I are rapidly degraded from the NH₂-terminus in type II diabetic patients and in healthy subjects. *Diabetes* 44: 1126–1131, 1995.
- Donowitz M, Li X. Regulatory binding partners and complexes of NHE3. *Physiol Rev* 87: 825–872, 2007.
- Drucker DJ. The role of gut hormones in glucose homeostasis. *J Clin Invest* 117: 24–32, 2007.
- Drucker DJ, Philippe J, Mojsov S, Chick WL. Glucagon like peptide I stimulates insulin gene expression and increases cyclic AMP levels in a rat islet cell line. *Proc Natl Acad Sci USA* 84: 3434–3438, 1987.
- Eng J, Kleinman WA, Singh L, Singh G, Raufman JP. Isolation and characterization of exendin-4, an exendin-3 analogue from *Heloderma suspectum* venom. *J Biol Chem* 267: 7402–7405, 1992.
- Fan L, Wiederkehr MR, Collazo R, Wang H, Crowder LA, Moe OW. Dual mechanisms of regulation of Na/H exchanger NHE-3 by parathyroid hormone in rat kidney. *J Biol Chem* 274: 11289–11295, 1999.
- Girardi AC, Degray BC, Nagy T, Biemesderfer D, Aronson PS. Association of Na^+/H^+ exchanger isoform NHE3 and dipeptidyl peptidase IV in the renal proximal tubule. *J Biol Chem* 276: 46671–46677, 2001.
- Girardi AC, Fukuda LE, Rossoni LV, Malnic G, Rebouças NA. Dipeptidyl peptidase IV inhibition downregulates Na^+/H^+ exchanger NHE3 in rat renal proximal tubule. *Am J Physiol Renal Physiol* 294: F414–F422, 2008.
- Girardi AC, Knauf F, Demuth H, Aronson PS. Role of dipeptidyl peptidase IV in regulating activity of Na^+/H^+ exchanger isoform NHE3 in proximal tubule cells. *Am J Physiol Cell Physiol* 287: C1238–C1245, 2004.
- Göke R, Fehmann HC, Linn T, Schmidt H, Krause M, Eng J, Göke B. Exendin-4 is a high potency agonist and truncated exendin-(9–39)-amide an antagonist at the glucagon-like peptide 1-(7–36)-amide receptor of insulin-secreting beta-cells. *J Biol Chem* 268: 19650–19655, 1993.
- Gromada J, Rorsman P, Dissing S, Wulff BS. Stimulation of cloned human glucagon-like peptide 1 receptor expressed in HEK 293 cells induces cAMP-dependent activation of calcium-induced calcium release. *FEBS Lett* 373: 182–186, 1995.
- Gronborg M, Kristiansen TZ, Stensballe A, Andersen JS, Ohara O, Mann M, Jensen ON, Pandey A. A mass spectrometry-based proteomic approach for identification of serine/threonine-phosphorylated proteins by enrichment with phospho-specific antibodies. *Mol Cell Proteomics* 517–527, 2002.
- Gutzwiller JP, Hruz P, Huber AR, Hamel C, Zehnder C, Drewe J, Gutmann H, Stanga Z, Vogel D, Beglinger C. Glucagon-like peptide-1 is involved in sodium and water homeostasis in humans. *Digestion* 73: 142–150, 2006.
- Gutzwiller JP, Tschopp S, Bock A, Zehnder CE, Huber AR, Kreyenbuehl M, Gutmann H, Drewe J, Henzen C, Goetze B, Beglinger C. Glucagon-like peptide 1 induces natriuresis in healthy subjects and in insulin-resistant obese men. *J Clin Endocrinol Metab* 89: 3055–3061, 2004.

21. Herrera C, Morimoto C, Blanco J, Mallol J, Arenzana F, Lluís C, Franco R. Comodulation of CXCR4 and CD26 in human lymphocytes. *J Biol Chem* 276: 19532–19539, 2001.
22. Hirata K, Kume S, Araki S, Sakaguchi M, Chin-Kanasaki M, Isshiki K, Sugimoto T, Nishiyama A, Koya D, Haneda M, Kashiwagi A, Uzu T. Exendin-4 has an anti-hypertensive effect in salt-sensitive mice model. *Biochem Biophys Res Commun* 380: 44–49, 2009.
23. Holst JJ. The physiology of glucagon-like peptide 1. *Physiol Rev* 87: 1409–1439, 2007.
24. Honegger KJ, Capuano P, Winter C, Bacic D, Stange G, Wagner CA, Biber J, Murer H, Hernando N. Regulation of sodium-proton exchanger isoform 3 (NHE3) by PKA and exchange protein directly activated by cAMP. *Proc Natl Acad Sci USA* 103: 803–808, 2006.
25. Hopsu-Havu VK, Glenner GG. A new dipeptide naphthylamidase hydrolyzing glycyl-prolyl-beta-naphthylamide. *Histochemie* 7: 197–201, 1966.
26. Houslay MD, Kolch W. Cell-type specific integration of cross-talk between extracellular signal-regulated kinase and cAMP signaling. *Mol Pharmacol* 58: 659–668, 2000.
27. Hu MC, Fan L, Crowder LA, Karim-Jimenez Z, Murer H, Moe OW. Dopamine acutely stimulates Na⁺/H⁺ exchanger (NHE3) endocytosis via clathrin-coated vesicles: dependence on protein kinase A-mediated NHE3 phosphorylation. *J Biol Chem* 276: 26906–26915, 2001.
28. Hull RN, Cherry WR, Weaver GW. The origin and characteristics of a pig kidney cell strain, LLC-PK. *In Vitro* 12: 670–677, 1976.
29. Kähne T, Neubert K, Faust J, Ansoorge S. Early phosphorylation events induced by DPIV/CD26-specific inhibitors. *Cell Immunol* 189: 60–66, 1998.
30. Kieffer TJ, McIntosh CH, Pederson RA. Degradation of glucose-dependent insulinotropic polypeptide and truncated glucagon-like peptide 1 in vitro and in vivo by dipeptidyl peptidase IV. *Endocrinology* 136: 3585–3596, 1995.
31. Kocinsky HS, Dynia DW, Wang T, Aronson PS. NHE3 phosphorylation at serines 552 and 605 does not directly affect NHE3 activity. *Am J Physiol Renal Physiol* 293: F212–F218, 2007.
32. Kocinsky HS, Girardi AC, Biemesderfer D, Nguyen T, Mentone S, Orłowski J, Aronson PS. Use of phospho-specific antibodies to determine the phosphorylation of endogenous Na⁺/H⁺ exchanger NHE3 at PKA consensus sites. *Am J Physiol Renal Physiol* 289: F249–F258, 2005.
33. Kurashima K, Yu FH, Cabado AG, Szabo EZ, Grinstein S, Orłowski J. Identification of sites required for down-regulation of Na⁺/H⁺ exchanger NHE3 activity by cAMP-dependent protein kinase phosphorylation-dependent and independent mechanisms. *J Biol Chem* 272: 28672–28679, 1997.
34. Lambeir AM, Durinx C, Scharpé S, De Meester I. Dipeptidyl-peptidase IV from bench to bedside: an update on structural properties, functions, and clinical aspects of the enzyme DPP-IV. *Crit Rev Clin Lab Sci* 40: 209–294, 2003.
35. Larsen PJ, Fledelius C, Knudsen LB, Tang-Christensen M. Systemic administration of the long-acting GLP-1 derivative NN2211 induces lasting and reversible weight loss in both normal and obese rats. *Diabetes* 50: 2530–2539, 2001.
36. Lowry OH, Rosebrough NJ, Farr AL, Randall RG. Protein measurement with the Folin phenol reagent. *J Biol Chem* 193: 265–275, 1951.
37. Mentlein R. Dipeptidyl-peptidase IV (CD26)—role in the inactivation of regulatory peptides. *Regul Pept* 85: 9–24, 1999.
38. Moe OW, Amemiya M, Yamaji Y. Activation of protein kinase A acutely inhibits and phosphorylates Na/H exchanger NHE-3. *J Clin Invest* 96: 2187–2194, 1995.
39. Moreno C, Mistry M, Roman RJ. Renal effects of glucagon-like peptide in rats. *Eur J Pharmacol* 434: 163–167, 2002.
40. Orłowski J, Grinstein S. Diversity of the mammalian sodium/proton exchanger SLC9 gene family. *Pflügers Arch* 447: 549–565, 2004.
41. Schlatter P, Beglinger C, Drewe J, Gutmann H. Glucagon-like peptide 1 receptor expression in primary porcine proximal tubular cells. *Regul Pept* 141: 120–128, 2007.
42. Schulteis PJ, Clarke LL, Meneton P, Miller ML, Soleimani M, Gawanis LR, Riddle TM, Duffy JJ, Doetschman T, Wang T, Giebisch G, Aronson PS, Lorenz JN, Shull GE. Renal and intestinal absorptive defects in mice lacking the NHE3 Na⁺/H⁺ exchanger. *Nat Genet* 19: 282–285, 1998.
43. Serre V, Dolci W, Schaefer E, Scrocchi L, Drucker D, Efrat S, Thorens B. Exendin-(9-39) is an inverse agonist of the murine glucagon-like peptide-1 receptor: implications for basal intracellular cyclic adenosine 3',5'-monophosphate levels and beta-cell glucose competence. *Endocrinology* 139: 4448–4454, 1998.
44. Shioda T, Kato H, Ohnishi Y, Tashiro K, Ikegawa M, Nakayama EE, Hu H, Kato A, Sakai Y, Liu H, Honjo T, Nomoto A, Iwamoto A, Morimoto C, Nagai Y. Anti-HIV-1 and chemotactic activities of human stromal cell-derived factor 1alpha (SDF-1alpha) and SDF-1beta are abolished by CD26/dipeptidyl peptidase IV-mediated cleavage. *Proc Natl Acad Sci USA* 95: 6331–6336, 1998.
45. Thum A, Hupe-Sodmann K, Göke R, Voigt K, Göke B, McGregor GP. Endoproteolysis by isolated membrane peptidases reveal metabolic stability of glucagon-like peptide-1 analogs, exendins-3 and -4. *Exp Clin Endocrinol Diabetes* 110: 113–118, 2002.
46. Tsuganezawa H, Preisig PA, Alpern RJ. Dominant negative c-Src inhibits angiotensin II induced activation of NHE3 in OKP cells. *Kidney Int* 54: 394–398, 1998.
47. Vallon V, Schwark JR, Richter K, Hropot M. Role of Na⁺/H⁺ exchanger NHE3 in nephron function: micropuncture studies with S3226, an inhibitor of NHE3. *Am J Physiol Renal Physiol* 278: F375–F379, 2000.
48. Wang T, Yang CL, Abbiati T, Schulteis PJ, Shull GE, Giebisch G, Aronson PS. Mechanism of proximal tubule bicarbonate absorption in NHE3 null mice. *Am J Physiol Renal Physiol* 277: F298–F302, 1999.
49. Weintraub WH, Machen TE. pH regulation in hepatoma cells: roles for Na-H exchange, Cl-HCO₃ exchange, and Na-HCO₃ cotransport. *Am J Physiol Gastrointest Liver Physiol* 257: G317–G327, 1989.
50. Wu MS, Biemesderfer D, Giebisch G, Aronson PS. Role of NHE3 in mediating renal brush border Na⁺-H⁺ exchange. Adaptation to metabolic acidosis. *J Biol Chem* 271: 32749–32752, 1996.
51. Yu M, Moreno C, Hoagland KM, Dahly A, Ditter K, Mistry M, Roman RJ. Antihypertensive effect of glucagon-like peptide 1 in Dahl salt-sensitive rats. *J Hypertens* 21: 1125–1135, 2003.
52. Zhang Y, Mircheff AK, Hensley CB, Magyar CE, Warnock DG, Chambrey R, Yip KP, Marsh DJ, Holstein-Rathlou NH, McDonough AA. Rapid redistribution and inhibition of renal sodium transporters during acute pressure natriuresis. *Am J Physiol Renal Fluid Electrolyte Physiol* 270: F1004–F1014, 1996.
53. Zhao H, Wiederkehr MR, Fan L, Collazo RL, Crowder LA, Moe OW. Acute inhibition of Na/H exchanger NHE-3 by cAMP. Role of protein kinase A and NHE-3 phosphoserines 552 and 605. *J Biol Chem* 274: 3978–3987, 1999.

Copyright of American Journal of Physiology: Renal Physiology is the property of American Physiological Society and its content may not be copied or emailed to multiple sites or posted to a listserv without the copyright holder's express written permission. However, users may print, download, or email articles for individual use.